

Depth and Density of the Antarctic Firn Layer

Michiel van den Broeke

*Institute for Marine and Atmospheric Research (IMAU), Utrecht University, Princetonplein 5, Utrecht 3584CC, Netherlands
broeke@phys.uu.nl

Abstract

The depth and density of the Antarctic firn layer is modeled, using a combination of regional climate model output and a steady-state firn densification model. The modeled near-surface climate (temperature, wind speed, and accumulation) and the depth of two critical density levels (550 kg m^{-3} and 830 kg m^{-3}) agree well with climate and firn density observations selected from >50 Antarctic coring sites ($r = 0.90\text{--}0.99$, $p < 0.0001$). The wide range of near-surface climate conditions in Antarctica forces a strong spatial variability in the depth and density of the Antarctic firn pack. In the calm, dry, and very cold interior, densification is slow and the firn-layer thickness exceeds 100 m and the firn age at pore close-off 2000 years. In the windier, wetter, and milder coastal zone, densification is more rapid and the firn layer shallower, typically 40–60 m, and younger, typically <50 years.

DOI: 10.1657/1523-0430(07-021)[BROEKE]2.0.CO;2

Introduction

A dry firn layer covers the largest part of the Antarctic ice sheet (Fig. 1). Firn represents the intermediate stage between fresh snow and glacial ice, and has a density between that of the surface snow (in Antarctica typically 350 kg m^{-3}) and glacial ice (typically 900 kg m^{-3}). In the strict sense of the word, firn is wetted snow that has survived summer melting without being transformed to ice, but here we include multi-year Antarctic snow in its definition. In the absence of significant melting, firn densification rate in Antarctica depends mainly on snow temperature, burial rate (surface accumulation), and near-surface wind speed. Below approximately 15 m depth, densification occurs at constant temperature, equal to the annual mean surface temperature. The different stages of densification of dry firn, i.e. settling up to a density of 550 kg m^{-3} and sublimation, diffusion, and deformation at higher densities, have been extensively described in literature. Firn densification models based on physical principles were proposed already several decades ago (Maeno, 1983; Alley, 1987; Wilkinson, 1988). Semi-empirical steady-state dry firn densification models were proposed by, among others, Herron and Langway (1980), Pimienta and Duval (1987), Kameda et al. (1994), Arnaud et al. (1998), Craven and Allison (1998), and Spencer et al. (2001).

Owing to the wide range of (near) surface climate conditions, the Antarctic firn layer is highly variable in depth and density (Craven and Allison, 1998; Kaspers et al., 2004; Li and Zwally, 2004; Zwally et al., 2005). To illustrate these differences, Figure 2 shows measured firn density profiles from the South Pole, representative of the calm, dry, and cold interior, and Byrd, representative of a windier, wetter, and milder near-coastal climate (for locations, see Fig. 1). At the South Pole, densification is slow, and the firn-layer thickness exceeds 100 m. At Byrd, densification is more rapid, and the firn layer shallower, typically 40–60 m. In regions with active katabatic winds and low precipitation rates, the firn layer may have been completely removed by snowdrift erosion and/or sublimation, exposing the glacier ice at the surface (Winther et al., 2001; van den Broeke et al., 2006).

In this paper we use output of a regional atmospheric climate model RACMO2/ANT in combination with a steady-state firn

densification model to study the spatial variability of the depth and density of the Antarctic firn layer. This paper updates previous work presented by Kaspers et al. (2004) by using improved fields of accumulation, near-surface wind speed and surface temperature, and a more extensive validation data set.

Model Description

FIRN DENSIFICATION MODEL

Kaspers et al. (2004) tested several empirical firn densification models for a range of Antarctic climate conditions and found good results for the models of Herron and Langway (1980), Pimienta and Duval (1987), and Arnaud et al. (1998). To improve the match for the deeper layers, Barnola et al. (1991) advocated the use of the Herron and Langway (1980) expression from the surface to the critical density level of 550 kg m^{-3} , and the Pimienta and Duval (1987) expressions further down. We follow their approach below the surface, but instead of imposing a fixed density value we added a surface density calculation based on annual average surface temperature, accumulation, and wind speed (adjusted from Kaspers et al., 2004). Next, the density model is integrated downwards from the surface to the depth where the approximate density of glacier ice (900 kg m^{-3}) is reached.

ATMOSPHERIC MODEL

The steady-state firn densification model requires annual average surface temperature (T_s), accumulation (A), and 10 m wind speed (V_{10}) as input values. These fields are taken as 25-year averaged output (1980–2004) from a regional atmospheric climate model that is specifically adapted for use over Antarctica (RACMO2/ANT). The horizontal resolution of RACMO2/ANT is 55 km, which determines the resolution of the density calculations. At the lateral boundaries the model is forced by European Centre for Medium-Range Weather Forecasts (ECMWF) reanalysis for the period January 1980–September 2002 (ERA40) and operational analyses for the period October 2002–December 2004. Sea ice cover and sea surface temperature are prescribed from ERA40. We use an accumulation distribution

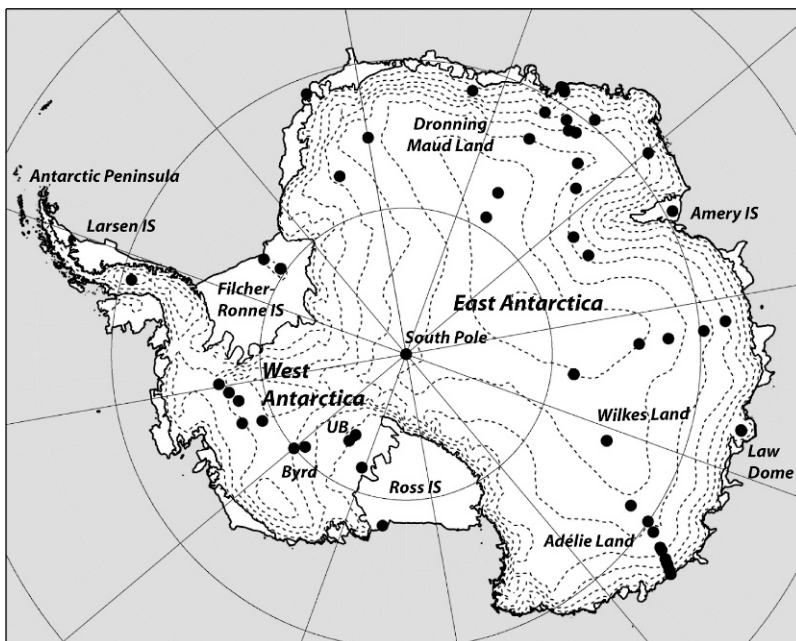


FIGURE 1. Map of Antarctica with main topographical features and location of firn coring sites. Dashed lines represent 500 m height contours. Abbreviations: IS = Ice Shelf, UB = Upstream B.

that takes into account in a simple fashion sublimation and erosion by snowdrift (van den Broeke et al., 2006).

Model Validation

NEAR-SURFACE CLIMATE

RACMO2/ANT provides a good representation of the Antarctic near-surface climate and mass balance, as previously shown by van Lipzig et al. (2004), Reijmer et al. (2005), and van de Berg et al. (2006). This is independently confirmed in Figures 3a–3c, where the (near) surface climate of RACMO2/ANT is

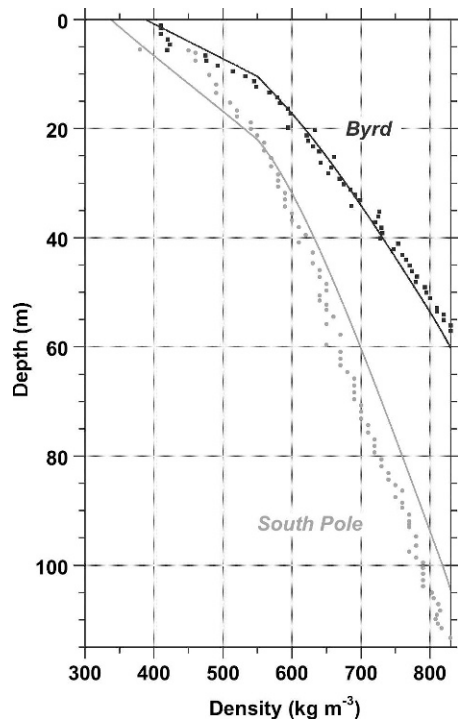


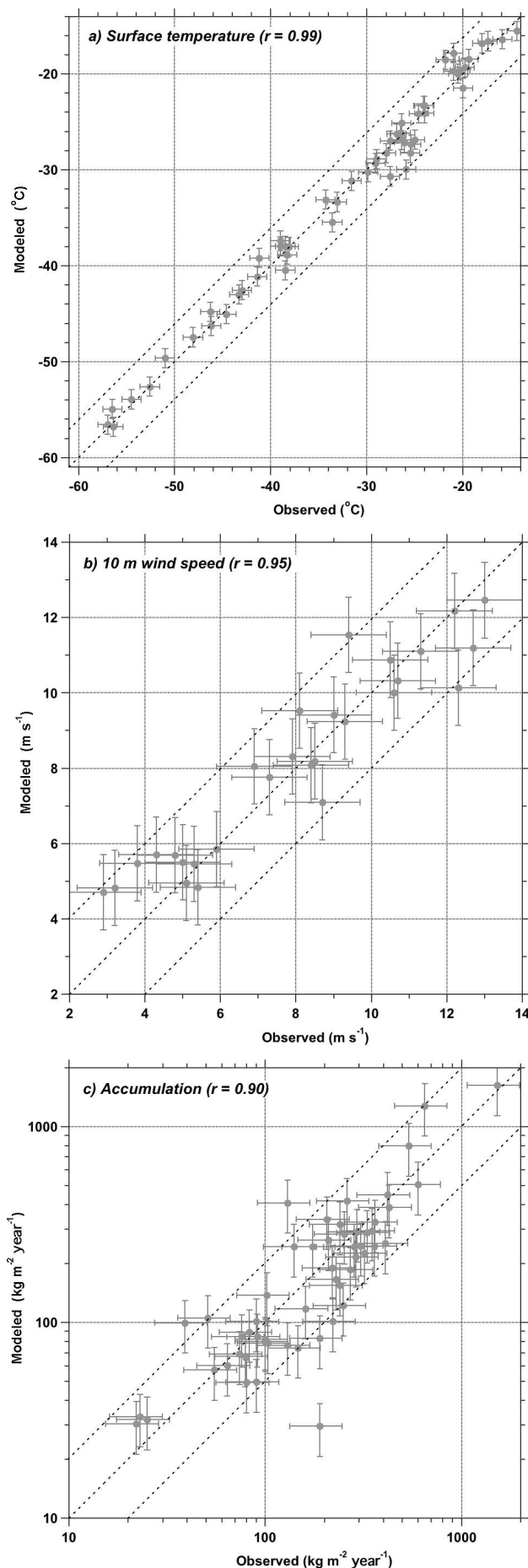
FIGURE 2. Example profiles of observed (dots) and modeled (lines) profiles of firn density at South Pole and Byrd stations.

validated using measurements of surface temperature T_s , 10 m wind speed V_{10m} , and accumulation A (whenever available) from >50 Antarctic firn sampling sites (for locations see Fig. 1). When necessary, wind speeds were extrapolated towards 10 m height assuming a neutral atmosphere and a value of 0.1 mm for surface momentum roughness. A cold bias of 2 K in modeled T_s was removed prior to plotting in Figure 3a and was corrected before the density calculations. We liberally assigned 1 K, 1 m s^{-1} , and 30% error bars to observed T_s , V_{10m} , and A with similar errors for the modeled values arising from the calculation and interpolation procedures.

After removal of the cold bias, temperature deviations are randomly distributed and follow the 1:1 line very well (Fig. 3a; $N = 64$, $r = 0.99$, $p < 0.0001$). The same is true for 10 m wind speed (Fig. 3b, $N = 35$, $r = 0.95$, $p < 0.0001$), apart from the fact that RACMO2/ANT slightly overestimates low and underestimates high wind speeds (Fig. 3b). This can be explained by the dominance of katabatic forcing in combination with slightly smoothed model topography. Accumulation is a very complex process in Antarctica and depends on solid precipitation, surface and snowdrift sublimation, and snow redistribution by the wind. This makes accumulation difficult to measure and model reliably, as local non-resolved processes and/or topography may play an important role in the accumulation distribution. Nevertheless, RACMO2/ANT reliably captures the strong accumulation gradients (Fig. 3c; $N = 62$, $r = 0.90$, $p < 0.0001$), with only few real outliers (van de Berg et al., 2006). In conclusion, RACMO2/ANT gives a faithful representation of the near-surface climate in Antarctica over a wide range climate conditions, making it a useful tool to drive a firn densification model.

FIRN DENSITY

Modeled and observed density profiles were compared for sites where the surface climate is sufficiently well simulated by RACMO2/ANT. We used the criteria that (corrected) annual mean model T_s , V_{10m} , and accumulation A are within 4 K, 2 m s^{-1} and a factor of 2 to observed values, respectively, as indicated by the dashed lines in Figures 3a–3c. This resulted in the rejection of one site for V_{10m} , five for A , and none for T_s . In



addition, we excluded two sites situated on ice shelves (where melting occurs) and one site with a known smooth (glazed, blue ice) surface, where snow accumulation is significantly reduced due to poor settling of fresh snow, a process not included in RACMO2/ANT. Moreover, we excluded one site where the absolute accumulation error exceeded $300 \text{ kg m}^{-2} \text{ yr}^{-1}$.

For the remaining sites, whenever available, we compared observed to modeled surface density and the depth of two critical density levels $\rho = 550 \text{ kg m}^{-3}$, representing the transition from settling to sintering as the dominant densification process, and $\rho = 830 \text{ kg m}^{-3}$, representing a proxy for the pore close-off density. We assume that if the surface density and the depth of these two levels are reliably simulated, the intermediate values are sufficiently well constrained. This is confirmed in Figure 2, where the lines show the modeled density profiles.

Figure 4a shows that, although reasonably well modeled, surface density shows large scatter ($N = 49$, $r = 0.81$, $p < 0.0001$). This comparison is of limited significance, mainly because surface density is a poorly defined quantity; the thickness of the sampled layer can be anything between 10 and 50 cm, but is seldom archived in metadata. Moreover, surface density may depend on the time of year, which adds more noise to the data. The range of observed values ($300\text{--}450 \text{ kg m}^{-3}$) is otherwise well captured by the model ($320\text{--}470 \text{ kg m}^{-3}$).

Figure 4b shows that the wide range of depths of the $\rho = 550 \text{ kg m}^{-3}$ level is also well modeled ($N = 45$, $r = 0.98$, $p < 0.0001$). The observed depths range between 6 and 26 m; the modeled range is 4 to 29.5 m. The largest deviations are found in the lower ranges, where the model tends to systematically underestimate the 550 kg m^{-3} depth.

Figure 4c shows that the wide range of depths of the $\rho = 830 \text{ kg m}^{-3}$ level is also well modeled ($N = 34$, $r = 0.94$, $p < 0.0001$). The observed depth of the $\rho = 830 \text{ kg m}^{-3}$ level ranges between 34 and 115 m, while modeled values range between 46 and 115 m. An outlier in the lower depth ranges is Upstream B, located at the origin of Ice Stream B in West Antarctica (Alley and Bentley, 1988). The value of 34 m at Upstream B is the lowest value reported to date from the dry snow zone of Antarctica. The anomalously rapid densification at Upstream B may be caused by horizontal compression from longitudinal stresses in the upper part of the ice stream flow, which obviously is not taken into account in our calculations. Another process that is neglected in the calculations is layer stretching, but this does not appear to negatively influence the results.

Based on this comparison we conclude that using regional climate model output to drive a steady-state firn density model yields sufficiently accurate results. Especially encouraging is that the large range of density and depth values is well captured, which justifies a more detailed study of the spatial variability of the Antarctic firn pack in the following section.

Spatial Variability of Antarctic Climate and Firn Density

NEAR-SURFACE CLIMATE

Figure 5 shows modeled distribution of surface temperature (a), 10 m wind speed (b), and accumulation (c). The surface temperature lapse rate along the ice sheet surface in East

←

FIGURE 3. Comparison of modeled and observed annual mean surface temperature (a), 10 m wind speed (b), and annual accumulation (c) at selected Antarctic firn coring sites.

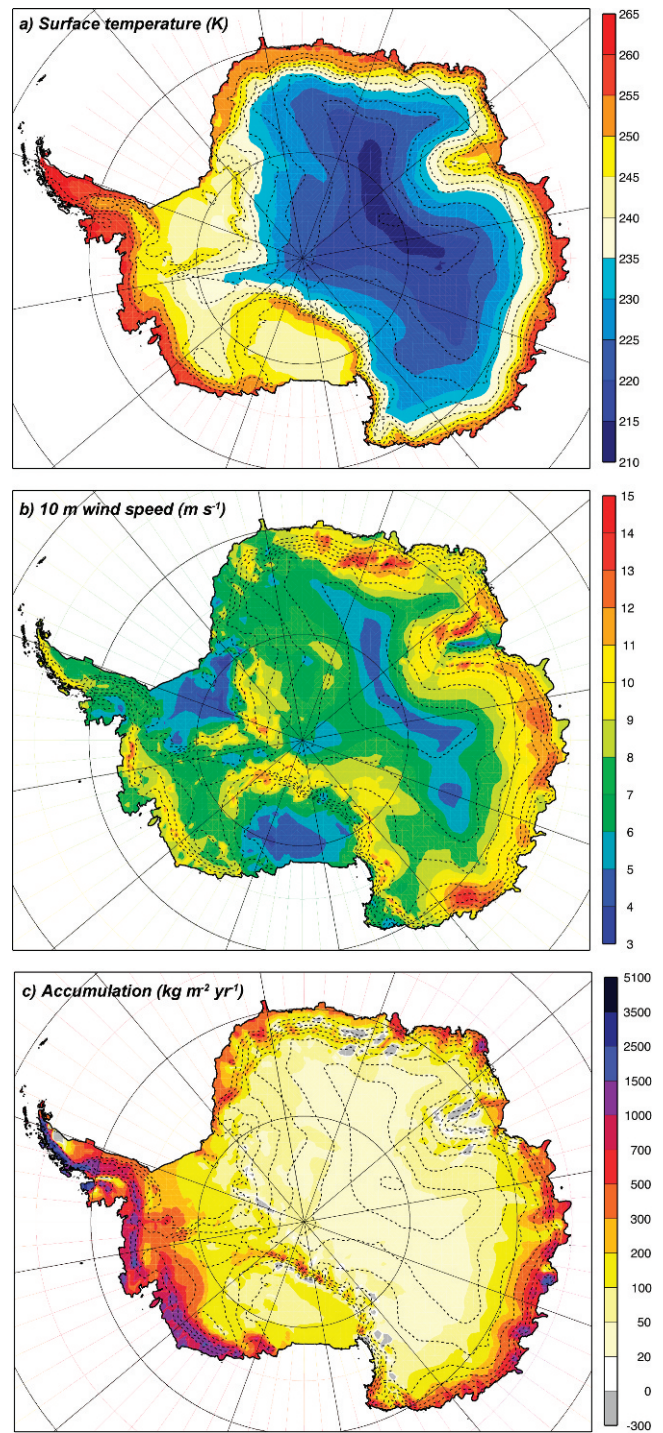
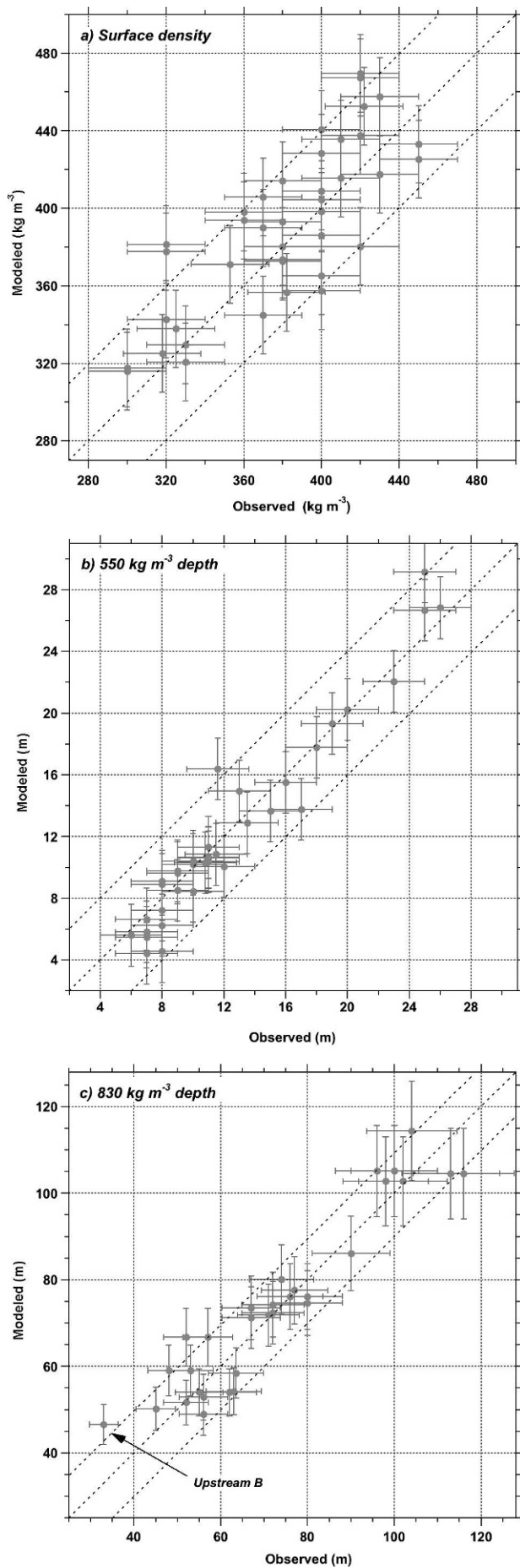


FIGURE 5. Modeled annual mean surface temperature (a), 10 m wind speed (b), and annual accumulation (c).

Antarctica is super-adiabatic (more than 9.8 K km^{-1} cooling), which is caused by the increasing surface-based wintertime temperature inversion towards the interior plateau (Fig. 5a). The temperature inversion in the coastal regions is weaker, because the

FIGURE 4. Comparison of modeled and observed surface density (a), and depth of the critical density levels 550 kg m^{-3} (b) and 830 kg m^{-3} (c) at selected Antarctic firn coring sites.

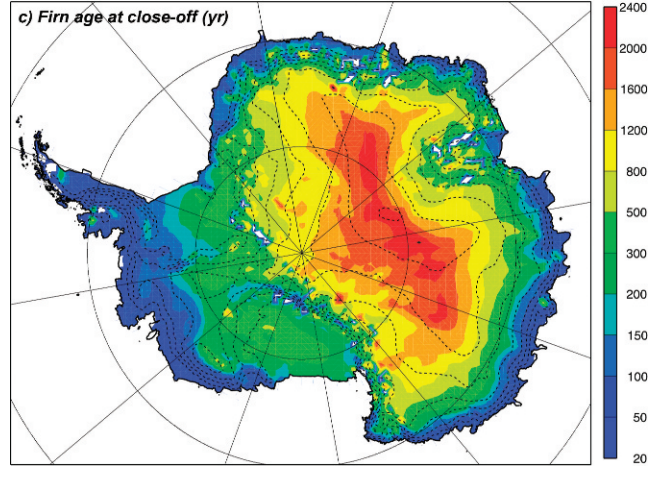
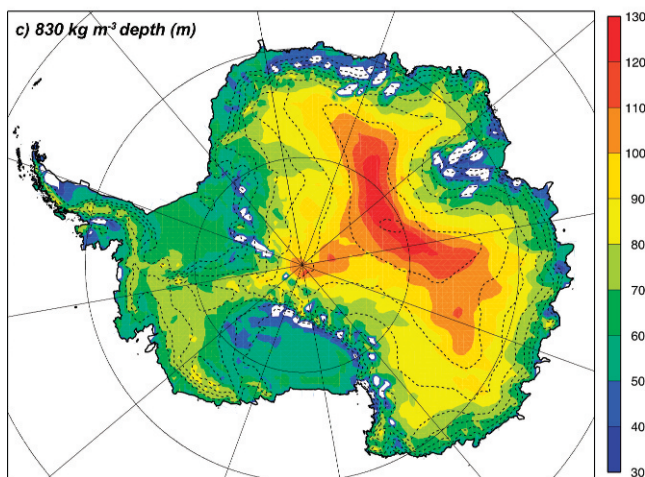
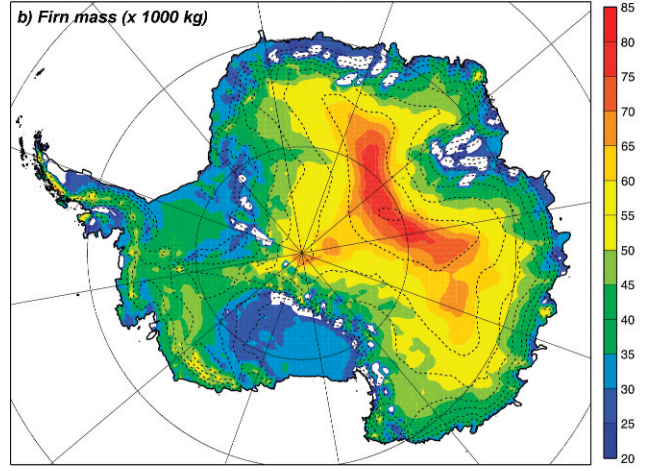
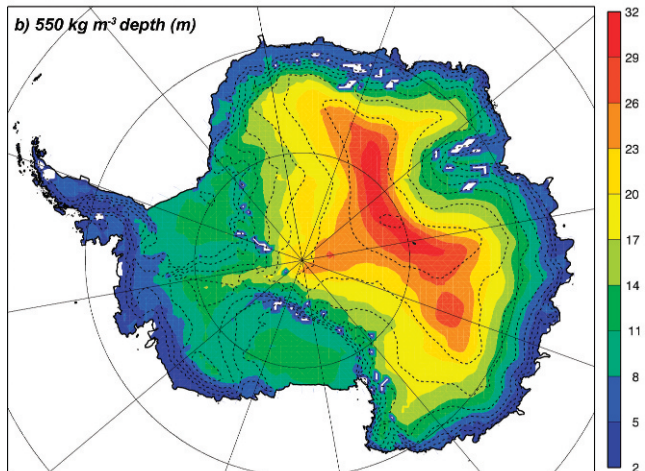
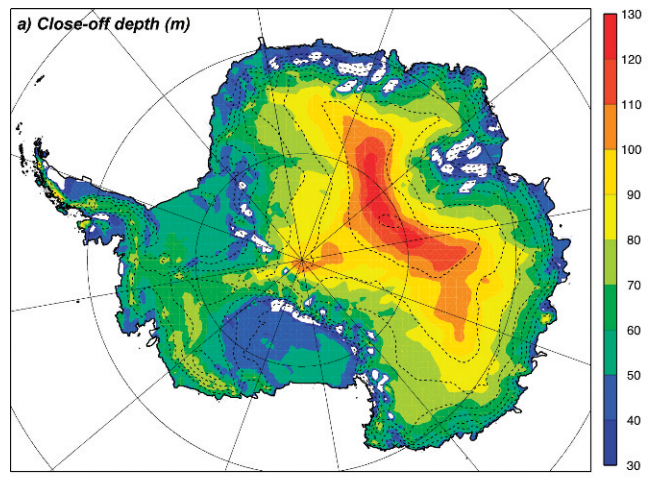
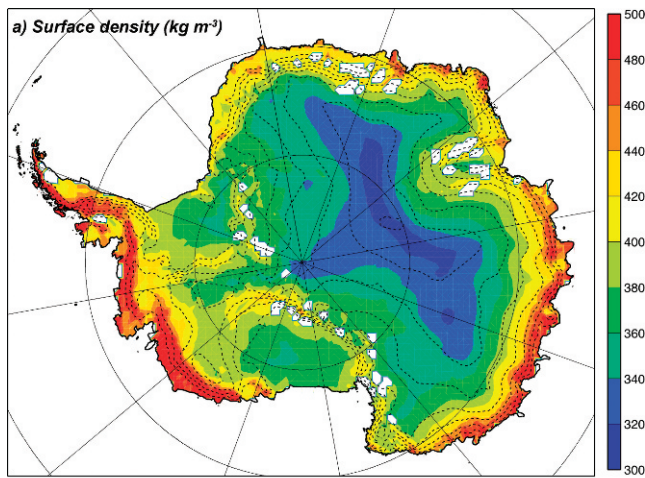


FIGURE 6. Modeled surface density (a), and depth of the critical density levels 550 kg m^{-3} (b) and 830 kg m^{-3} (c).

FIGURE 7. Modeled depth of pore close-off (a), firn mass above pore close-off (b), and age of firn at pore close-off (c).

radiation balance is less negative, owing to more clouds, and turbulent mixing in the boundary layer is stronger owing to stronger katabatic winds.

The increase in near-surface wind speed from the interior plateau to the coast is clearly visible in Figure 5b and is caused primarily by enhanced katabatic forcing over the steeper coastal slopes. The dominance of the katabatic forcing is underlined by the low annual mean wind speeds over the interior domes and the Ross and Filchner-Ronne ice shelves, where a significant surface slope and thus katabatic forcing is absent. Important longitudinal

variations in wind speed occur in response to variations in the ice sheet topography. The large-scale pressure gradient, which is generally directed in the downslope direction, tends to enhance the katabatic wind in coastal East Antarctica. This influence reaches a maximum around the 2500 m a.s.l. height contour in East Antarctica, which results in strong near-surface winds reaching quite far into the ice sheet interior (van den Broeke et al., 2002; van den Broeke and van Lipzig, 2003).

Snowfall in Antarctica is mainly driven by forced convection, i.e. relatively warm and moist air that is forced onto the ice sheet. As a result, accumulation decreases strongly from the coast inland, as

do temperature and wind speed (Fig. 5c, note the nonlinear scale). In addition there are important longitudinal accumulation gradients caused by the interaction of the easterly coastal flow and the ice sheet topography. A vivid example is the area around Law Dome, with accumulation rates $>1500 \text{ kg m}^{-2} \text{ yr}^{-1}$ on the eastern slopes and $<200 \text{ kg m}^{-2} \text{ yr}^{-1}$ on the western side. Similarly strong precipitation shadow effects can be found all along the Antarctic coastline at various spatial scales. In dry regions, surface and snowdrift sublimation and snowdrift erosion may exceed the solid precipitation flux, resulting in areas with negative surface mass balance (ablation, colored gray in Fig. 5c). In these regions, the firn layer may be completely removed so that glacier ice is exposed at the surface. Antarctic accumulation is discussed in detail by van de Berg et al. (2006), the mechanisms leading to the formation of Antarctic ablation areas by van den Broeke et al. (2006).

FIRN DENSITY

Figure 6 shows the modeled distributions of surface density (a), and depths of the density levels 550 kg m^{-3} (b) and 830 kg m^{-3} (c). Surface density (Fig. 6a) has values ranging from 300 kg m^{-3} in the interior to $>450 \text{ kg m}^{-3}$ in the coastal region, where a combination of strong winds, high accumulation, and high temperatures is found. Surface density is smaller in the center of the large ice shelves compared to the margins, as a result of the low interior temperatures and wind speeds.

The modeled depth of the 550 kg m^{-3} density level (Fig. 6b) mostly reflects variations in the surface density, as we would intuitively expect for the depth interval where settling is the dominant densification mechanism. The modeled range of values (2–32 m) is very large and can be explained by the strong climate gradients from coast to interior as discussed in the previous section. The exception of a monotonous decrease in depth of the 550 kg m^{-3} density level is found on the large ice shelves, where interior values (11–14 m) are higher than the values near the edges (typically 8–11 m).

The modeled depth of the 830 kg m^{-3} density level (Fig. 6c) does not show a monotonous decrease from the interior towards the ice sheet margin. High coastal burial rates tend to increase the depth of this density level, which reaches minimum values of 40–50 m in regions where the ice sheet merges with ice shelves, in e.g. Dronning Maud Land, the Larsen ice shelf in the Antarctic Peninsula and the western margin of the Ross ice shelf. These regions have in common that they are dry and relatively warm (föhn effect), conditions that are favorable for fast sintering in the deeper firn layers and hence faster metamorphosis towards ice density. In wetter coastal regions, the 830 kg m^{-3} density level is reached typically between 50 and 70 m but higher/lower values are found locally associated with accumulation anomalies, see e.g. Law Dome. In interior West Antarctica and along the spine of the Antarctic Peninsula, values of 70–80 m are found, while values in excess of 100 m are common in interior East Antarctica above 3000–3500 m a.s.l.

CHARACTERISTICS AT PORE CLOSE-OFF DEPTH

Figure 7 shows depth (a), total overlying weight (b), and firn age (c) at the level at which pore close-off is predicted. Kaspers et al. (2004) empirically modeled the density at which the pores close off as a function of surface temperature and accumulation. This yields values close to or somewhat lower than 830 kg m^{-3} , resulting in pore close-off depths slightly shallower than the 830 kg m^{-3} density level (compare Figs. 7a and 6c). The patterns of variability are similar.

The total mass of the firn column ranges between 20,000 and $>80,000 \text{ kg m}^{-2}$ (Fig. 7b) and correlates strongly with close-off depth, which suggests that the average density of the firn layer does not vary much. Indeed, average firn density of the layer that extends from the surface to close-off depth typically varies less than 5% from a mean value of 650 kg m^{-3} , with values ranging from 625 kg m^{-3} in the eastern Ross Ice Shelf to 675 kg m^{-3} in high accumulation coastal areas (not shown).

If we divide firn mass by accumulation, we retrieve the firn age at pore close-off depth (Fig. 7c). The combination of strongly increasing firn depth and decreasing accumulation towards the interior leads to a range of firn ages that spans over two orders of magnitude. Pore close-off firn age can be as low as 20 yr in warm, windy, and wet coastal areas. In the calm, dry, and cold interior, firn ages at close-off depth typically exceed 2000 years. These data are useful for the interpretation of the age difference between gas in air bubbles and the surrounding ice (delta age). In the near future, a gas diffusion model will be used to calculate the firn-gas age difference at pore close-off depth under present-day climate conditions.

Conclusions

We modeled the depth and density of the Antarctic firn layer, driving a steady-state firn densification model with output of a regional atmospheric climate model. Comparison with *in situ* climate parameters and density observations at >50 firn sampling sites shows modeled and observed near-surface climate and firn density in good agreement. The very large climate gradients force a wide range of firn densities in Antarctica. Surface density is predicted to vary between 300 kg m^{-3} in the cold and dry interior ice sheet, where near-surface wind speed is low, and $>450 \text{ kg m}^{-3}$ in the windy, wet, and relatively warm coastal ice sheet. The level at which the 550 kg m^{-3} value is reached varies from 3 to 32 m, the 830 kg m^{-3} level from 30 to 130 m, but the latter does not decrease monotonously towards the coast. Instead, the lowest values of pore close-off depth are found in dry and relatively warm regions, often in the lee side of topographical obstructions where the föhn effect is active. As the average firn density from the surface to pore close-off is relatively constant across the ice sheet, the weight of the firn column shows comparable variability from 20,000 to $85,000 \text{ kg m}^{-2}$. As a combined effect of the accumulation and firn depth gradients, the firn age at pore close-off varies two orders of magnitude across Antarctica, from close to 20 years in the coastal zone to >2000 years in the far interior. Part of the agreement of the steady-state model and observations may come from the co-variability of accumulation, wind, and temperature in Antarctica. That is why future work will focus on the time-dependent firn densification process, which will also enable us to assess the contribution of temporal temperature and accumulation variability on ice sheet elevation changes through firn densification.

Acknowledgments

We thank Willem Jan van de Berg and Erik van Meijgaard for modeling support.

References Cited

- Alley, R. B., 1987: Firn densification by firn boundary sliding. *Journal de Physique*, 48: 249–256.
- Alley, R. B., and Bentley, C. R., 1988: Ice-core analysis on the Siple coast of west Antarctica. *Annals of Glaciology*, 11: 1–7.

- Arnaud, L., Lipenkov, V. Y., Barnola, J.-M., Gay, M., and Duval, P., 1998: Modelling of the densification of polar firn: characterization of the snow-firn transition. *Annals of Glaciology*, 26: 39–44.
- Barnola, J.-M., Pimienta, P., Raynaud, D., and Korotkevich, Y. S., 1991: CO₂-climate relationship as deduced from the Vostok ice core: a re-evaluation of the air dating. *Tellus*, 43(B): 83–90.
- Craven, M., and Allison, I., 1998: Firnification and the effects of wind-packing on Antarctic snow. *Annals of Glaciology*, 27: 239–245.
- Herron, M., and Langway, C., Jr., 1980: Firn densification: an empirical model. *Journal of Glaciology*, 25: 373–385.
- Kameda, T., Shoji, H., Kawada, K., Watanabe, O., and Clausen, H. B., 1994: An empirical relation between overburden pressure and firn density. *Annals of Glaciology*, 20: 87–94.
- Kaspers, K. A., van de Wal, R. S. W., van den Broeke, M. R., van Lipzig, N. P. M., and Brenninkmeijer, C. A. M., 2004: Model calculations of the age of firn air across the Antarctic continent. *Atmospheric Chemistry and Physics*, 4: 1817–1853.
- Li, J., and Zwally, H. J., 2004: Modeling the density variation in the shallow firn layer. *Annals of Glaciology*, 38: 303–313.
- Maeno, N., 1983: Sintering of ice and its implication to the densification of snow at polar glaciers and ice sheets. *Journal of Physical Chemistry*, 87: 4103.
- Pimienta, M., and Duval, P., 1987: Rate controlling processes in the creep of polar glacier ice. In *Proceedings VIIth Symposium of Physics and Chemistry of Ice*, Grenoble 1–5 Sep. 1985. *Journal de Physique*, 48: 243–248.
- Reijmer, C. H., van Meijgaard, E., and van den Broeke, M. R., 2005: Evaluation of temperature and wind over Antarctica in a regional atmospheric climate model. *Journal of Geophysical Research*, 110: D04103, doi: 10.1029/2004JD005234.
- Spencer, M. K., Alley, R. B., and Creyts, T. T., 2001: Preliminary firn-densification model with 38-site dataset. *Journal of Glaciology*, 47(159): 671–676.
- van de Berg, W. J., van den Broeke, M. R., van Meijgaard, E., and Reijmer, C. H., 2006: Reassessment of the Antarctic surface mass balance using calibrated output of a regional atmospheric climate model. *Journal of Geophysical Research*, 111: D11104, doi: 10.1029/2005JD006495.
- van den Broeke, M. R., and van Lipzig, N. P. M., 2003: Factors controlling the near-surface wind field in Antarctica. *Monthly Weather Review*, 131: 733–743.
- van den Broeke, M. R., van Lipzig, N. P. M., and van Meijgaard, E., 2002: Momentum budget of the East-Antarctic atmospheric boundary layer: results of a regional climate model. *Journal of the Atmospheric Sciences*, 59: 3117–3129.
- van den Broeke, M. R., van de Berg, W. J., van Meijgaard, E., and Reijmer, C. H., 2006: Identification of Antarctic ablation areas using a regional atmospheric climate model. *Journal of Geophysical Research*, 111: D18110, doi: 10.1029/2006JD007127.
- van Lipzig, N. P. M., Turner, J., Colwell, S. R., and van den Broeke, M. R., 2004: The near-surface wind field over the Antarctic continent. *International Journal of Climatology*, 24(15): 1973–1982.
- Wilkinson, D. S., 1988: A pressure sintering model for the densification of polar firn and glacier ice. *Journal of Glaciology*, 34(115): 40–45.
- Winther, J.-G., Jespersen, M. N., and Liston, G. E., 2001: Blue-ice areas in Antarctica derived from NOAA AVHRR satellite data. *Journal of Glaciology*, 47: 325–334.
- Zwally, H. J., Giovinetto, M. B., Li, J., Cornejo, H. G., Beckley, M. A., Brenner, A. C., Saba, J. L., and Yi, D., 2005: Mass changes of the Greenland and Antarctic ice sheets and shelves and contributions to sea-level rise: 1992–2002. *Journal of Glaciology*, 51(175): 509–527.

Ms accepted September 2007